8704–8713 *Nucleic Acids Research, 2016, Vol. 44, No. 18* *Published online 20 June 2016*
doi: 10.1093/nar/gkw559

Overexpression of eIF5 or its protein mimic 5MP perturbs eIF2 function and induces *ATF4* translation through delayed re-initiation

Caitlin Kozel[1,2,†], Brytteny Thompson[1,†], Samantha Hustak[1,†], Chelsea Moore[1,†], Akio Nakashima[3], Chingakham Ranjit Singh[1], Megan Reid[1], Christian Cox[1], Evangelos Papadopoulos[4], Rafael E. Luna[4], Abbey Anderson[1], Hideaki Tagami[5], Hiroyuki Hiraishi[1], Emily Archer Slone[1], Ken-ichi Yoshino[3], Masayo Asano[1], Sarah Gillaspie[1], Jerome Nietfeld[2], Jean-Pierre Perchellet[1], Stefan Rothenburg[1], Hisao Masai[6], Gerhard Wagner[4], Alexander Beeser[1], Ushio Kikkawa[3], Sherry D. Fleming[1] and Katsura Asano[1,*]

[1]Molecular Cellular Developmental Biology Program, Division of Biology, Kansas State University, Manhattan, KS 66506, USA, [2]College of Veterinary Medicine, Kansas State University, Manhattan, KS 66506, USA, [3]Biosignal Research Center, Kobe University, Kobe 657-8501, Japan, [4]Department of Biological Chemistry and Molecular Pharmacology, Harvard Medical School, Boston, MA 02115, USA, [5]Graduate School of Natural Sciences, Nagoya City University, Nagoya 467-8501, Japan and [6]Genome Dynamics Project, Department of Genome Medicine, Tokyo Metropolitan Institute of Medical Science, Tokyo 156-8506, Japan

Received March 30, 2016; Revised June 07, 2016; Accepted June 10, 2016

ABSTRACT

ATF4 is a pro-oncogenic transcription factor whose translation is activated by eIF2 phosphorylation through delayed re-initiation involving two uORFs in the mRNA leader. However, in yeast, the effect of eIF2 phosphorylation can be mimicked by eIF5 overexpression, which turns eIF5 into translational inhibitor, thereby promoting translation of *GCN4*, the yeast *ATF4* equivalent. Furthermore, regulatory protein termed eIF5-mimic protein (5MP) can bind eIF2 and inhibit general translation. Here, we show that 5MP1 overexpression in human cells leads to strong formation of 5MP1:eIF2 complex, nearly comparable to that of eIF5:eIF2 complex produced by eIF5 overexpression. Overexpression of eIF5, 5MP1 and 5MP2, the second human paralog, promotes ATF4 expression in certain types of human cells including fibrosarcoma. 5MP overexpression also induces ATF4 expression in *Drosophila*. The knockdown of 5MP1 in fibrosarcoma attenuates ATF4 expression and its tumor formation on nude mice. Since 5MP2 is overproduced in salivary mucoepidermoid carcinoma, we propose that overexpression of eIF5 and 5MP induces translation of *ATF4* and potentially other genes with uORFs in their mRNA leaders through delayed re-initiation, thereby enhancing the survival of normal and cancer cells under stress conditions.

Being the major energy consuming process, mRNA translation is tightly regulated (1). Many of the specific mRNA targets of translational regulation include those encoding transcription factors, thereby allowing rapid cellular signaling involving global transcriptional changes. One example is *ATF4* mRNA, which encodes a pro-oncogenic transcription factor (2) and whose translation is controlled through special arrangement of two uORFs, uORF1 and uORF2, found in its leader region. In contrast to the canonical translation wherein the ribosome dissociates from mRNA after translation termination, the ribosome resumes scanning after uORF1 translation. Under normal conditions, the ribosome commits to re-initiate at uORF2, inhibiting downstream re-initiation at *ATF4*. However, when certain stress signals come in, the ribosome pre-initiation complex (PIC) does not assemble before the uORF2 start

*To whom correspondence should be addressed. Tel: +785 532 0116; Email: kasano@ksu.edu
†These authors contributed equally to this paper as the first authors.
Present addresses:
Hiroyuki Hiraishi, Immuno-Biological Laboratories, Co. Ltd., Fujioka 375-0005, Japan.
Alexander Beeser, Culver-Stockton College Science Center, Canton, MO 63435, USA.

codon, resulting in the bypass of uORF2, but the PIC assembles before the downstream start codon for *ATF4*, thereby inducing *ATF4* translation (3).

The choice of the re-initiation site at uORF2 or *ATF4* start codon is ultimately determined by the availability of the translation initiation factor eIF2, an essential PIC component that delivers Met-tRNA$_i^{Met}$ to the ribosome in a GTP-dependent manner. In human, four eIF2α kinases (eIF2αK), PKR, PERK, GCN2 and HRI, phosphorylate eIF2 at Ser 51 of its α subunit, thereby inhibiting its activation by guanine nucleotide exchange, and delaying PIC assembly. Activation of PERK and GCN2 is known to induce *ATF4* translation. However, in yeast, any perturbation of other eIF activity or expression that results in inhibiting eIF2 is shown to induce translation of *GCN4*, the yeast equivalent of *ATF4*, whose mRNA leader also contains the paired uORFs. For example, overexpression turns eIF5, a canonical translation factor and binding partner of eIF2, into the inhibitor of the initiator tRNA binding to the ribosome, thereby mimicking the effect of eIF2 phosphorylation and inducing *GCN4* (4). Furthermore, overexpression of the protein mimic and inhibitor for eIF5, termed eIF5-mimic protein 1 (5MP1), was reported to induce *ATF4* translation in mouse embryonic fibroblasts with an eIF2α Ser 51-to-Ala mutation (5). This finding suggests the presence of alternative pathways for translational induction of *ATF4* through expression of a translational inhibitory protein. Because the overexpression of 5MP2/BZW1, the second human paralogue of 5MP, appears to be responsible for salivary mucoepidermoid carcinogenesis (6), the alternative pathways may be important for various biological processes including tumorigenesis.

eIF5 interacts with both GTP- and GDP-bound forms of eIF2. The eIF5 interaction with eIF2:GTP:Met-tRNA$_i^{Met}$ ternary complex occurs in the multifactor complex (MFC) with eIF1 and eIF3, promoting Met-tRNA$_i^{Met}$ recruitment to 40S ribosomal subunits (7,8). The eIF5 interaction with eIF2-GDP antagonizes the GDP/GTP exchange for the latter, thereby inhibiting translation (4,9). The crucial role eIF5 plays in controlling eIF2 function is not only established in yeast, but is strongly supported in the entire Eukarya by the existence of its protein mimic, 5MP. 5MP does not carry the GTPase activating function displayed by eIF5 (10), but possesses a W2-type CTD for eIF2 and eIF3 binding, similar to eIF5 (5). All eukaryotes except most protozoans, yeasts and nematodes contain 5MP (11). The two human copies, 5MP1 and 5MP2, are 70% identical to each other and expressed in cultured mammalian cells at a level stoichiometric to initiation factors (∼50–80% of eIF2 levels) (12).

Although the interaction between 5MP and eIF2 and the competition between 5MP and eIF5 for eIF2 have been demonstrated *in vitro* (5,11), the interaction between 5MP and eIF2 has not been demonstrated or even compared to the interaction between eIF5 and eIF2 in human cells. Curiously, the current proteomics databases do not list any interaction between 5MP and eIF2 or between 5MP and any other translation initiation factor. We generated plasmids to overexpress human eIF5 and 5MP and compared their abilities to bind eIF2 and other initiation factors and to induce *ATF4* in human cells. We find that human 5MP1 binds eIF2 and induces *ATF4* similarly to eIF5. Furthermore, we show that 5MP1 facilitates ATF4 expression in fibrosarcoma and promotes its tumorigenesis. Our studies reveal a common molecular basis for general translation inhibition by eIF5 and 5MP overexpression, as well as for specific translational induction of *ATF4* through these stimuli.

MATERIALS AND METHODS

Cell culture and transfection

Human embryonic kidney (HEK) 293T (ATCC), HeLa sh-PKR and shCtrl (kindly provided by Charles Samuel) (13), human fibrosarcoma HT1080 (ATCC), and *Drosophila melanogaster* S2 cells were grown and transfected and HT1080 cell lines stably expressing sh 5MP1 or sh GFP were generated and maintained, all as described in Supplementary text. To express His$_6$- and FLAG-tagged eIF5, 5MP1 and 5MP2, we cloned human cDNAs encoding them under the EF1A promoter, generating pEF1A derivatives (see Supplementary text for details). We also generated a pEF1A-heIF5 derivative carrying the Quad mutation H305D/N306D/E347K/E348K, known to abolish eIF5 binding to eIF2β and eIF1 (14).

Affinity purification and MS

Transfection of HEK293T with the pEF1A derivatives and subsequent affinity purification were done as described previously (15), with modifications described in Supplementary file. Complex I and II fractions were subjected for SDS-PAGE, followed by silver staining. Complex I proteins ranging from 35 to 75 kDa were analyzed separately in three gel pieces (Supplementary Table S1), while complex II proteins in the whole lane were analyzed in 12 gel pieces (Figures 2, 3 and Supplementary Figure S2). In-gel digestion of protein bands and the MS analysis of the products were performed as described (16), except that the analysis of complex II fractions used C18 reverse-phase chromatography (ADVANCE UHPLC, AMR) and a quadrapole ion trap mass spectrometer (LTQ Orbitrap Velos Pro; Thermo Fisher Scientific) with a Advanced Captive Spray SOURCE mounted on a three-dimensional stage (AMR). For complex I fractions, peptide fragments were applied to a nanoflow high-performance liquid chromatography system (Paradigm MS4; Michrom Bioresources, Auburn, CA, USA) equipped with an L-column ODS (150 mm length × 100 μm ID, particle size of 3 μm, CERI, Tokyo, Japan) and analyzed with an LTQ-Orbitrap Discovery mass spectrometer (ThermoFisher Scientific).

For semi-quantitative analysis of MS data, we used the output files of Cut-off 30. We used emPAI as a proxy for molar amount of proteins found in MS samples, as defined as follows:

$$emPAI = 10^{\frac{N_{\text{observed}}}{N_{\text{observable}}}} - 1$$

where N_{observed} (N_{obd}) is the number of peptides detected in the experiment and $N_{\text{observable}}$ (N_{oble}) is the number of peptides theoretically detected per protein molecule (17). Although $N_{\text{obd}}/N_{\text{oble}}$ values (PAI) are considered as the hallmark of molecular amounts detected in the MS experiment,

comparison of this value and the known amount for 46 purified proteins indicated that the value correlated most highly with logarithm of protein amount (r = 0.89) with deviation factor (average ± S.D.) = 1.6 ± 0.5 (17). Thus, emPAI (rather than N_{obd}/N_{oble} = PAI) is the best proxy for relative molecular amount of the protein present in the MS sample. Assuming that eIF2, eIF2B, eIF3 and the ribosomal subunits bound to the FLAG-tagged 5MP1 or eIF5 as a holo complex, the average total emPAI values computed for individual protein subunits throughout each lane were employed as the relative molar amounts of each complex in the complex II fractions and presented in Table 1. The significance of protein association is judged by two criteria: (i) Absence of relevant peptides in the vector-transfected sample. (ii) If peptides derived from a protein complex are present in the vector-transfected sample, *P*-value is computed with total emPAI values for measurement from each subunit of the complex.

Luciferase reporter assay

Cells are transfected with a fixed ratio of a ATF4-firefly luciferase plasmid and control *Renilla* luciferase plasmid, together with the eIF5 or 5MP expression plasmid, and subjected for Dual Glo^R Luciferase Assay (Promega), as described in detail in Supplementary text. For expression in human cells, we used *TK-ATF4-luc*, its derivative carrying a mutation altering the uORF1 or uORF2 start codon (3) or fusing uORF2 in-frame with the *luc* gene (K.A., personal collection) for the firefly construct and the control *Renilla* luciferase plasmid (3). As a control for *ATF4* induction, cells were treated with 250 nM thapsigargin (Tg) for 16–20 h prior to the assay. For expression in insect cells, we used *D. melanogaster ATF4-luc* plasmid p1696 for the firefly construct and pAc5.1C-RLuc-V5His6 (18) for the *Renilla* construct.

Fibrosarcoma experiments

Five homozygous male nude mice (NU/J, Jackson Laboratory) were used. Animals were housed and cared within the temperature-controlled the Division of Biology animal facility at Kansas State University. Mice were maintained in a 12:12 light:dark cycle and specific pathogen free facility (*Helicobacter sp*., mouse hepatitis virus, minute virus of mice, mouse parvovirus, Sendai virus, murine norovirus, *Mycoplasma pulmonis*, Theiler's murine encephalomyelitis virus and endo- and ecto- parasites). Food and water were provided *ad libitum.* All animal experiments were performed in accordance with NIH guidelines and with the approval of the KSU Institutional Animal Care and Use Committee. Nude mice were subcutaneously injected with clone 5.3 (HT1080 sh5MP1) cells in their left flank, while all mice received injections of negative control HT1080 in their right flank. Cells (2×10^6) were mixed with equal volume of matrigel and injected in 200 μl volumes. When the total diameters of tumors in both franks were ∼1.5 cm, mice were euthanized and tumors were excised, photographed, weighed and embedded in OCT freezing medium. OCT frozen samples are sectioned at 8 μm, stained by hematoxilyn and eosin and subjected to pathological analysis.

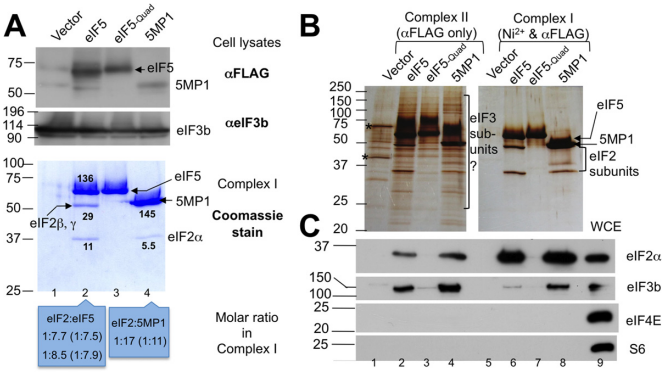

Figure 1. Complex formation by eIF5 and 5MP1 in human cells. (**A**) Double affinity purification of eIF5:eIF2 or 5MP1:eIF2 complexes (Complex I). Top two gels show the immunoblots of the whole cell extracts (WCE) with antibodies indicated to the right. In the third gel, complexes purified from vector-treated (lane 1) or cells expressing His/FLAG-eIF5 (lane 2), eIF5-Quad mutant (lane 3), or 5MP1 (lane 4) were stained by Coomassie blue. Numbers beside each gel indicate the location of protein size standards in kDa. Numbers beside each band are the amounts of proteins quantified by densitometric scanning in an arbitrary unit. Boxes on the bottom indicate molar ratios of eIF2 to 5MP1 or eIF5. For eIF5, the ratio was computed twice from eIF2β/γ and eIF2α bands and presented on top and bottom, respectively. For 5MP1, this was computed from the eIF2α band. Values in parenthesis are those obtained from another independent experiment. (**B** and **C**) Single αFLAG affinity purified complex of eIF5 and 5MP1 (Complex II) contains eIF2 and eIF3. (B) Silver staining and (C) immunoblots of 2.5% complexes II (lanes 1–4) and 8% complex I fractions (lanes 5–8) from cells with indicated treatments are presented with the position of protein size markers (in kDa). In (C), 0.3% of WCE from vector-treated cells was analyzed together (lane 9). Detected proteins are listed to the right of the blots. *, components of the PRMT5:MET50 complex, specifically found in the vector-treated sample (see Supplementary text for details).

Statistical analysis

We used Student's *t*-test to obtain *P*-values. Bars in the graphs denote SEM.

RESULTS

eIF5 and 5MP1 interact with eIF2 and eIF3 in human cells

To study 5MP interaction with initiation factors in human cells and the effect of its overexpression on ATF4 expression, we cloned human cDNAs encoding 5MP1 under a strong promoter (P_{eEF1A}) in a vector derived from CSII-EF-MCS (15) (pEF1A derivatives, see Materials and Methods and Supplementary Data). Similarly, we made expression plasmids for eIF5 or its mutant carrying the Quad mutation that abolishes eIF5 binding to eIF1 and eIF2 (14). The expressed proteins have the N-terminal His_6-tag and the C-terminal triple FLAG-tag, allowing nickel-αFLAG double affinity purification of these proteins. Transfection of these plasmids, along with the vector control, into HEK 293T cells, displayed roughly equivalent expression of FLAG-tagged proteins (Figure 1A, top two gels): Although 5MP1 expression tends to be lower than that of eIF5, eIF5-Quad mutant expressed to the level equivalent to the wild-type eIF5 (also see Figure 4A below). The expression of eIF5 and 5MP1 reduced protein synthesis, as measured by luciferase from a co-transfected constitutive reporter plasmid (Supplementary Figure S1). As a control, the treat-

Table 1. emPAI values for translation components associated with 5MP1 and eIF5 in complex II

Row	Protein name	Vector	5MP1	eIF5
1	FLAG-tagged protein		786	258
MFC components				
2	eIF2 [α, β, γ]	0.18 ± 0.08	94 ± 64#	45 ± 10#
3	eIF3 [a-m]	1.2 ± 0.2	7.0 ± 1.2*	1.4 ± 0.3
4	eIF1 (14 kDa)	0	4.0#	0
Other eIFs				
5	eIF1A (16 kDa)	0	4.4#	1.9#
6	eIF2B [α, β, γ, δ, ϵ]	0	5.4 ± 2.1#	1.8 ± 0.5*
7	eIF4G1 (176 kDa)	0.04	0.07	0.07
8	p97/NAT1/DAP5 (102 kDa)	0	1.1#	0.07#
9	eIF4B (70 kDa)	7.4	0.6	0.3
Ribosomal proteins				
10	Small subunit proteins [30]	2.9 ± 0.5	6.9 ± 1.2*	2.0 ± 0.3
11	Large subunit proteins [36]	0.77 ± 0.23	1.7 ± 0.4*	1.3 ± 0.4
PRMT5:MET50 complex				
12	PRMT5 (73 kDa)	26.2	0.05	0.1
13	MET50 (37 kDa)	6.78	0	0

The total emPAI values (17) for factor or ribosomal subunit indicated in column 1 are listed for vector-transfected, 5MP1 and eIF5 sample (columns 3–5). For entries of a single polypeptide, their sizes are listed in parentheses (column 2). SEM is shown for data with multiple subunits. The names (eIFs) or numbers (ribosomal subunits detected) of the subunits are shown in brackets. *, significant increases compared to the vector control sample ($P < 0.05$). #, specificity inferred from the absence of the relevant protein(s) in the vector control sample. See Supplementary text for proteins mainly found in the vector-transfected sample.

ment of vector-transfected cells with thapisgargin (Tg), a known translational inhibitor drug, strongly reduced luciferase synthesis (Supplementary Figure S1, column 1). The reduced luciferase synthesis confirms in human cells that 5MP1 is a general translation inhibitor (5) and that eIF5 overexpression turns eIF5 into an inhibitor of translation (4).

The double affinity purification of the FLAG/His_6-tagged proteins from HEK293T cell transfectants (see Materials and Methods for details) yielded purified samples of the expressed proteins and co-purifying proteins (Complex I in Figure 1A and B). eIF5 and 5MP1, but not eIF5-Quad mutant, were co-purified with a 35-kDa protein, which was identified as the α subunit of eIF2 by Western blotting (with anti-eIF2α) (Figure 1C) and mass spectrometry (MS) (Supplementary Table S1). MS also identified the β and γ subunits of eIF2 as co-purifying proteins for both eIF5 and 5MP1 (Supplementary Table S1); eIF2β and eIF2γ co-migrated with 5MP1 in the SDS-PAGE, and therefore could not be identified in this complex by the Coomassie or silver staining (Figure 1A and B). As expected, the eIF5-Quad mutation abolished eIF5 interaction with eIF2 (Figure 1A–C). Thus, eIF5 and 5MP1 interact with eIF2 in human cells at similar affinities, as expected from their similar *in vitro* binding affinities to eIF2β-NTT, the major substrate-binding site (11,14).

Immunoblotting detected trace amounts of eIF3b subunit in the eIF5 and 5MP1 complex I samples (Figure 1C, lanes 6 and 8). To better study the interaction of eIF5 and 5MP1 with other translation factors than eIF2, we purified the complexes by omitting the nickel affinity purification step, which may have inhibited interaction with them. The single αFLAG-affinity purification of both eIF5 and 5MP1 proteins yielded complexes containing, in addition to the eIF2 subunits, proteins with sizes ranging from ∼170 to ∼25 kDa (Complex II, Figure 1). These proteins are reminiscent of eIF3 subunits and distinct from non-specific pro-

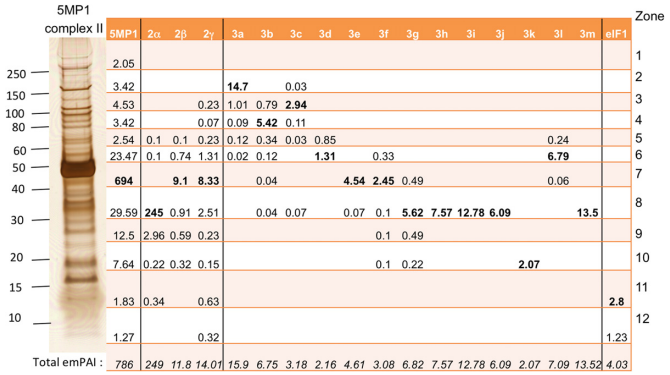

Figure 2. MS analysis of 5MP1 complex II. After SDS-PAGE and silver staining, gels were sliced into12 pieces, each of which was subjected for MS analysis. Table to the right summarizes emPAI values for proteins listed across the top. On the bottom, sum of emPAI values is listed as total "molar" amount associated with 5MP1.

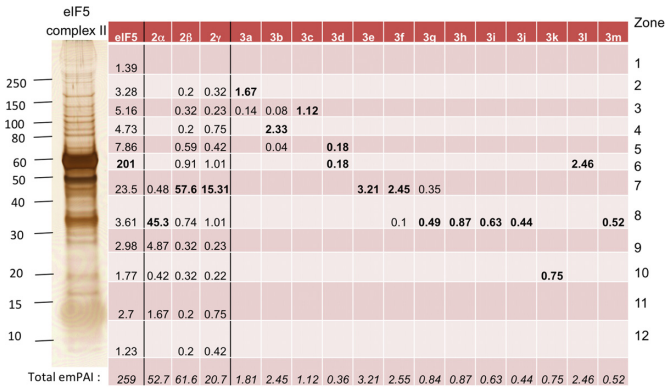

Figure 3. MS analysis of eIF5 complex II. emPAI values of detected proteins are listed as in Figure 2.

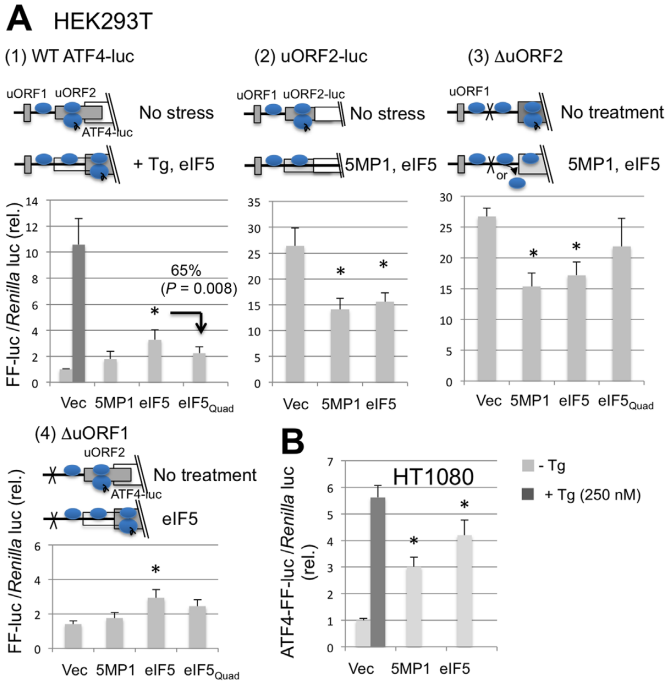

Figure 4. The effect of 5MP1 and eIF5 overexpression on *ATF4* translational control in HEK293T and HT1080. (**A**) HEK293T cells are transfected with 10:1:10 amounts of firefly luciferase plasmid (*ATF4-luc* [panel 1], uORF2-*luc* [panel 2] and *ATF4-luc* mutants altering start codon of uORF2 [panel 3] or uORF1 [panel 4]), a *Renilla* luciferase plasmid and a pEF1A derivative expressing indicated proteins or a vector control. After 2 days, cells were lysed to measure firefly and *Renilla* luciferase activities. Graph indicates the firefly/Renilla luciferase expression ratio normalized to the value for *ATF4-luc* vector control. For the experiment with *ATF4-luc*, a portion of vector control transfectants was treated with 250 nM Tg for overnight, and the luciferase activity was presented in dark grey. *, significant changes compared to the value from vector control in each panel. Panel 1, $P = 0.017$ (n = 10). Panel 2, $P = 0.01$, 0.001 (n = 8). Panel 3, $P = 0.01$, 0.02 (n = 6). Panel 4, $P = 0.03$ (n = 6). Hooked arrow, a significant change (n = 8). (**B**) HT1080 cells are transfected similarly with *ATF4-luc* plasmid and assayed for luciferase activities. * $P < 0.02$, compared to the values from vector control in each panel (n = 4).

teins observed in the fraction from vector-transfected cells (lane 1, Figure 1B). Immunoblotting indeed confirmed that eIF3b is enriched in 5MP1 or eIF5 Complex II, compared to the amount of eIF2α. Thus, by omitting the nickel purification step, we were able to have more stable eIF3 association with eIF5 or 5MP1. Little or no eIF4E (a subunit of eIF4F cap-binding complex) or ribosomal protein S6 was found in all the samples tested (Figure 1C), in support of specificity of complex II purification. The Western blot also showed that eIF5 interaction with eIF3 depended on the intact Quad residues important for eIF5 interaction with eIF1 and eIF2β (14).

MS analysis of proteins associated with eIF5 and 5MP1

To elucidate the molecular composition of protein complexes associated with eIF5 and 5MP1, we performed MS on complexes II formed with these proteins (Figure 1C, lanes 2 and 4; Supplementary Figure S2, lanes 2–3), along with the fraction from vector transfected cells (Figure 1 and Supplementary Figure S2, lanes 1). For each sample, the whole lane was divided into 12 zones, each of which was subjected to MS. As shown in Supplementary Table S2, initial assessment of the MASCOT output file (the summary of the number of peptides observed per zone per protein species) revealed that many proteins were specifically found in complex II fractions of eIF5 and 5MP1 compared to proteins found in the vector-transfected fraction. Strikingly, 12 of the 17 proteins most specifically associated with eIF5 and 5MP1 were initiation factors – all three subunits of eIF2, a, b and c subunits of eIF3, all five subunits of eIF2B and p97/NAT1/DAP5 (Supplementary Table S2).

Of proteins found in complex with eIF5 and 5MP1, little or no peptides derived from eIF2 or eIF2B subunits or p97/NAT1/DAP5 were found in the fraction from vector-transfected cells, in support of the specificity of their association (Supplementary Table S2). However, significant numbers of peptides derived from eIF3 subunits were found in the vector-transfected fraction (Supplementary Table S2), even though these numbers appeared to be lower than those from eIF5 or 5MP1 complex II fractions. Because eIF3b was not detected in the vector-transfected fraction for eIF5 or 5MP1 complex II in the immunoblot shown in Figure 1 (also see Figure 8), it appears that a small fraction of eIF3 bound to the FLAG affinity column in this particular experiment (see Supplementary text for details).

Figures 2 and 3 summarize emPAI values for MFC components found in the 12 zones of complex II fractions with 5MP1 and eIF5, respectively, as proxies for their molar amounts. Most of the proteins listed here are found in the zones expected from their sizes. The bottom of the graph lists the sum of the proteins found in the whole lane, and hence considered to be the estimated amount of associated protein. Although total emPAI values for eIF2 and eIF3 subunits varied widely, they appeared to fall within the values expected for their presence in the same complex (eIF2 or eIF3) from previously determined correlation co-efficient (17). We confirmed, however, that the ratios of average emPAI value for eIF2 to that of eIF5 or 5MP1 in respective complexes (1:8.6 and 1:5.6) matches well with the ratio determined from Coomassie stained bands in Figure 1A (on average, 1:14 and 1:7.9, respectively). Importantly, the emPAI values for eIF3 subunit abundance in 5MP1 complex were significantly higher than the values in the control-treated sample ($P < 0.001$, n = 13; asterisk in Table 1, column 3). Because eIF1 was also detected specifically in 5MP1 complex II fraction (Figure 2 and Table 1), we conclude that 5MP1 is able to form an MFC-like complex with eIF1, eIF2 and eIF3 in place of eIF5. Though MS did not provide evidence for specific eIF5 binding to eIF3, all eIF3 subunits were detected in the eIF5 complex II fraction (Figure 3). Based on our western blot analysis in Figure 1C, we conclude that eIF5 forms a multifactor complex with eIF2 and eIF3, as reported previously (8).

The semi-quantitative analysis also supports the assessment that eIF5 and 5MP1 interact with eIF2B, the guanine nucleotide exchange factor for eIF2 (Table 1, row 6). These interactions might be bridged by eIF2, because the average emPAI values for the pentameric eIF2B complex were several-fold lower than those for eIF2 in both the complex II fractions (Table 1, rows 2 versus 6). Thus, the interaction with eIF2B appears to depend on the amount of eIF2

associated with eIF5 or 5MP1. A similar eIF5:eIF2:eIF2B complex has been observed in yeast when eIF5 was overexpressed (4), and is suggested to play a role in controlling the guanine nucleotide binding status of eIF2, with eIF5 serving as the guanine nucleotide dissociation inhibitor (GDI) (9,19). Our results present the first evidence that 5MP1 makes a ternary complex with eIF2 and eIF2B, in agreement with the model that 5MP1 can interact with GDP-bound eIF2 (5). Other new interactions found in this study, such as those with eIF1A (20) and p97/NAT1/DAP5 (Table 1, rows 5, 8), are discussed in the Supplementary text.

Overexpression of 5MP1 and eIF5 promotes ATF4 expression in human cells

Having observed specific interaction of 5MP1 and eIF5 with eIF2 and eIF3, the major MFC components, we examined the model that 5MP1 and eIF5 overexpression induces *ATF4* translation through inhibition of initiation factor assembly. To test this, we transfected the ATF4-firefly luciferase reporter plasmid with the paired uORFs (3), along with the pEF1A-based overexpression plasmid and a control *Renilla* luciferase plasmid. As shown in Figure 4A, panel 1, columns 3–4, we found that eIF5 overexrression induces ATF4 expression, dependent on its Quad residue. However, the level of *ATF4* induction was lower than the level induced by a medium dose (250 nM) of thapisgargin (Tg), the ER stress inducer that activates PERK eIF2α kinase (Figure 4A, panel 1, column 1). 5MP1 overexpression also did not significantly induce *ATF4* in this experiment (column 2).

In an effort to evaluate these findings, we performed assays using other reporter plasmids. The experiment with a uORF2-luciferase plasmid showed that both eIF5 and 5MP1 expression inhibited the uORF2 translation (Figure 4, panel 2). Thus, the uORF2 start codon appears to be bypassed not only by eIF5, as expected from increased ATF4-luc activity (Figure 4A, panel 1), but also by 5MP1. Provided that 5MP1 and eIF5 overexpression allows a strong bypass of uORF2 translation, why did not we observe strong *ATF4-luc* induction by these treatments? To address this, we performed experiments with mutant versions of the ATF4-luciferase plasmid, lacking the start codon of uORF2 (ΔuORF2; Figure 4, panel 3) or uORF1 (ΔuORF1; Figure 4, panel 4). The ΔuORF2 mutation eliminates the inhibitory effect of uORF2 and thereby confers a high ATF4-luciferase activity (27-fold compared to WT *ATF4-luc*) due to efficient re-initiation after uORF1 translation (Figure 4A, panel 3, column 1) (3). Importantly, 5MP1 or eIF5 overexpression suppressed the re-initiation at *ATF4* after uORF1 translation (Figure 4A, panel 3), perhaps owing to PIC dissociation from mRNA or even slower reacquisition of the eIF2 ternary complex (see the model in Figure 4A, panel 3). Moreover, the experiment with the ΔuORF1 mutant confirms that uORF2 is translated normally in the presence of overproduced 5MP1 or eIF5, inhibiting *ATF4* translation (Figure 4A, panel 4: for the small effect of eIF5 overexpression, see below). Therefore, the overexpressed eIF5 and 5MP1 can cause the ribosomal bypass of uORF2 after uORF1 translation, but this event does not appear to lead to strong *ATF4* re-initiation due to a secondary effect on PIC scanning. In regard to this point, the experiment in Figure 4A, panel 4 also showed a minor but significant increase in *ATF4* translation by eIF5 overexpression potentially through leaky scanning in the primary initiation event. This supports the idea that the secondary effect includes very slow TC reaquisition at least in the case of eIF5 overexpression.

Encouraged by these findings, we examined three more additional human cell lines, fibrosarcoma HT1080, HeLa cells in which PKR is stably knocked down by sh RNA (sh PKR), and its control expressing randomized RNA (sh Control) and the insect cells *Drosophila* S2. We used the fibrosacorma cell line HT1080, because the knockdown studies demonstrated that *ATF4* is responsible for its tumor growth *in vitro* and *in vivo* (21). The use of HeLa shPKR (13) was prompted by our previous finding that 5MP1 overexpression in mouse embryonic fibroblast *eIF2α-S51A*$^{-/-}$ mutant induces ATF4 expression, but not in WT MEF (5). Among the four human eIF2α kinases, we chose PKR for knockdown, because PKR may be activated during plasmid transfection in response to transfection reagents or strong RNA transcription from the transfected plasmid. The activated PKR may in turn repress translation of FLAG-tagged proteins from the transfected plasmids, thereby attenuating the effect of 5MP1 or eIF5 on *ATF4* induction.

As shown in Figures 4B and 5B panel 2, the overexpression of 5MP1 and eIF5 induced ATF4 expression in both HT1080 and HeLa shPKR cells, as expected. Furthermore, the effect of eIF5 depended on the Quad residues critical for its interaction with eIF1 and eIF2 (columns 3 and 4). In HeLa sh RNA control (shCtrl) cell lines, however, the *ATF4* induction by eIF5 was minor and smaller than that by 5MP1 (Figure 5B, panel 1). Compared to the assay in HeLa shCtrl, sh PKR treatment significantly increased the magnitude of *ATF4* induction by eIF5 overexpression ($P < 0.001$, $n = 9$; compare columns 3 in Figure 5B). The overall weaker effect of eIF5 and 5MP1 in shCtrl cells is apparently due to their lower expression levels compared to those in shPKR cells (Figure 5A), in agreement with the rationale as described above. We found that the *ATF4-luc* level is higher in shCtrl than in shPKR line (Figure 5C), suggesting that PKR is activated through transfection under the experimental conditions.

Paired uORFs suited for induction by eIF2 inhibition are found in the leader regions of all the *ATF4* mRNAs in Metaoza (except for nematodes). Though the 5MP knockdown decreased the transcription of an ATF4-dependent gene in the red flour beetle, *Tribolium castaneum* (11), a direct effect of 5MP on ATF4 expression has not be examined in insects. To test this, we generated *ATF4-luc* reporter using *ATF4* mRNA from *D. melanogaster (Dme)*. Control transfection with a luciferase plasmid indicates that expression of 5MP from *D. melanogaster* or *T. castaneum* (*Tca*, red flour beetle) strongly attenuates luciferase protein synthesis (Figure 6A and B). Conversely, experiments with the *Dme ATF4-luc* plasmid show that *Dme* and *Tca* 5MP expression induces ATF4 expression (Figure 6C and Supplementary Figure S3). Thus, 5MP is a translational inhibitor and specific inducer of *ATF4* in insects as well.

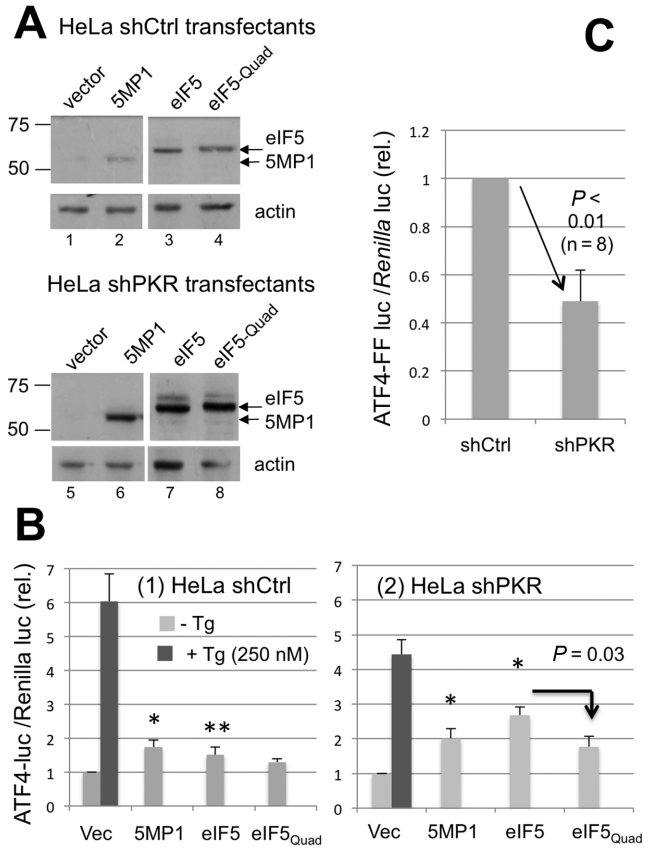

Figure 5. The effect of 5MP1 and eIF5 overexpression on *ATF4* translational control in HeLa cells knocked down for PKR eIF2αK. HeLa cells knocked down for PKR (shPKR, panel 1) or expressing a randominzed sh RNA (shCntrl, panel 2) are transfected with the *ATF4-luc* plasmid, the *Renilla* lucifereae plasmid and pEF1A derivatives, as in Figure 4A, panel 1, and assayed for ATF4-luciferease activity. (**A**) Immunoblot analysis of lysates from HeLa transfectants with indicated treatments. Top, anti-FLAG. Bottom, anti-actin. (**B**) Graph indicates *ATF4-luc*/*Renilla luc* expression ratio under expression of indicated proteins, relative to the value from vector control. *$P < 0.05$ compared to value with the vector control in each panel. Panel 1, $P = 0.007$ (n = 10). Panel 2, $P = 0.07$, $P < 0.0001$ (n = 10). **$P = 0.05$ (n = 10). Hooked arrow, a significant change (n = 7). (**C**) *ATF4-luc*/*Renilla luc* expression ratio was compared between vector-control experiments for HeLa shCtrl and shPKR lines that are done in parallel.

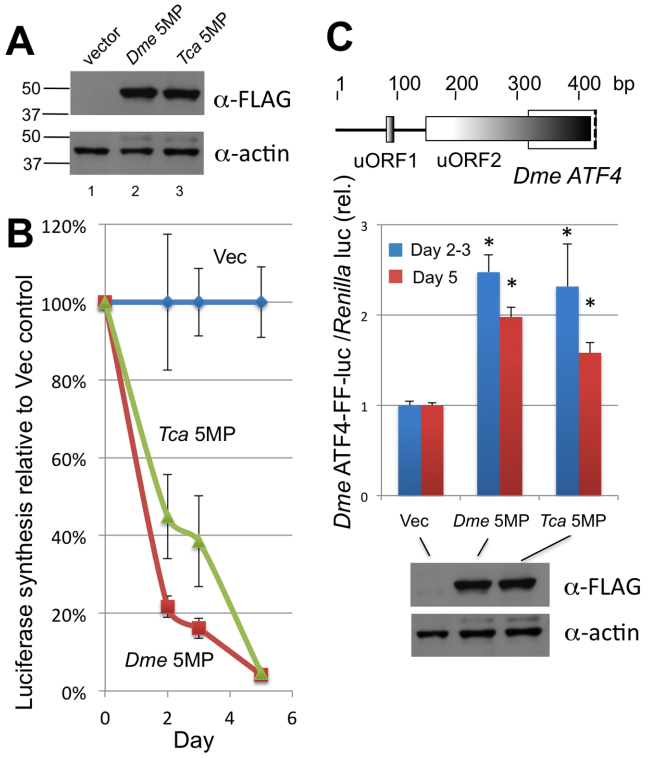

Figure 6. The effect of 5MP expression on translational control in insect cells. (**A** and **B**) *Drosophila* S2 cells were transfected with 5:1:25 amounts of pAc5.1C-Fluc-V5His6, pAc5.1C-Rluc-V5His6 and pAc-Dme5MP, pAc-Tca5MP or vector control (see Supplementary file for details). Expressed 5MP proteins are tagged with FLAG-epitope at their C-termini. After 2, 3 and 5 days, a portion of the cells are withdrawn for Western blotting with anti-FLAG and anti-actin (A) or dual firefly and *Renilla* luciferase assays. (A) Immunoblots with cells on day 3. Graph in (B) shows the firefly luciferase expression relative to the vector control for each experiment. Expression ratio of firefly and *Renilla* luciferase was unaltered by 5MP expression (Supplementary Figure S3). (**C**) Transfection of S2 cells was done as in (A) and (B) except with p1696 with *DmeATF4* leader region cloned between the actin promoter and luciferase coding region of pAc5.1C-Fluc-V5His6, in place of the Fluc plasmid. Transfected cells were analyzed as in (A) and (B). Graph indicates the firefly/Renilla expression ratio for transfectants expressing indicated proteins, relative to the vector control on day 2 and 3. *, significant changes compared to the vector control. Days 2–3, $P = 0.01$, 0.04 (n = 7). Day 5, $P = 0.003$, 0.02 (n = 4). Schematic on top shows the structure of *Dme ATF4* leader region. Immunoblot on the bottom shows experiment with p1696 transfectants on day 3, conducted in parallel with experiment in (A).

5MP1 promotes fibrosarcoma tumorigenesis

The finding that 5MP1 stimulates ATF4 expression in HT1080 promoted us to examine the role of 5MP1 in fibrosarcoma tumorigenesis (21). If the ATF4 expression at least partially depends on 5MP1, the 5MP1 knockdown is expected to compromise its tumorigenicity. We generated a stable HT1080 cell line knocked down for 5MP1 by an sh5MP1 plasmid, in which the level of 5MP1 was decreased by 45% (Figure 7A). As a control, we generated a stable transfectant of HT1080 expressing sh GFP RNA (shGFP). The resulting sh5MP1 clone termed 5.3 displayed reduced cell growth *in vitro*, compared to naïve HT1080 and HT1080 shGFP (Figure 7B) and a modest reduction in ATF4-luc expression, as examined with the *ATF4-luc* plasmid (Figure 7C). The magnitude of *ATF4* induction by Tg was not altered by sh5MP1, however (Figure 7C). These results indicate that 5MP1 knockdown reduces ATF4 expression in and *in vitro* growth of HT1080.

To verify the reduced expression of endogenous ATF4, we performed immunocytochemistry with anti-ATF4. As shown in Figure 7D, we observed predominant nuclear localization of ATF4 in naïve HT1080 (Figure 7D), and the anti-ATF4 signal was somewhat reduced in the clone 5.3 cells (Figure 7D). As shown in Figure 7E, our quantification showed that the anti-ATF4 signal per cell was reduced significantly to 78%, in agreement with reduced *ATF4-luc* transgene expression.

To examine the effect of sh5MP1 on tumor growth *in vivo*, we inoculated the clone 5.3 cells (2×10^6) into one hind flank of five nude mice. As controls, we inoculated the same number of naïve HT1080 into the opposite flank of

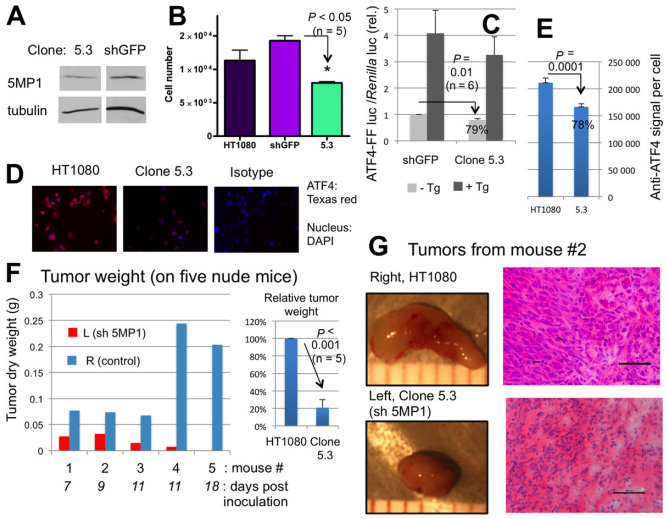

Figure 7. Fibrosarcoma HT1080 cells knocked down for 5MP1 display decreased ATF4 expression and tumorigenicity. Stable HT1080 transfectants expressing shRNA against 5MP1 (clone 5.3) and GFP (as a control) were generated and assayed as described in Material and Methods. (**A**) Immunoblot of lysates prepared from clone 5.3 (sh 5MP1) or sh GFP control. Equal protein amounts were loaded and treated with antibodies indicated to the left. (**B**) Cell titor assay was performed with naïve HT1080, clone 5.3 and shGFP control and presented in a graph. (**C**) Clone 5.3 and shGFP control lines were transfected with 10:1 amounts of the *ATF4-luc* and Renilla luciferase plasmids. On day 1, a portion of the cells was treated overnight with Tg (250 nM). On day 2, firefly and Renilla activities were assayed. Firefly:Renilla expression ratio was presented relative to the value with untreated shGFP cells. (**D** and **E**) Clone 5.3 and naïve HT1080 cells were stained with DAPI (blue) and anti-ATF4 (red). Isotype, mouse IgG was used for HT1080 as control. (**E**) Integral density of anti-ATF4 signal was quantified for 25 clone 5.3 and 30 HT1080 cells and presented. See Supplementary Method for details. (**F** and **G**) Clone 5.3 and naïve HT1080 cells were inoculated to left and right rear flanks of five nude mice. Left graph indicates the weight of tumors generated by these cells and collected after indicated times. Right graph shows the analysis of relative size of the tumors. (**G**) Isolated tumors (left) and hematoxilyn and eosin staining of the tumor sections (right). Arrows indicate dividing cells. Bar, 100 μm.

the same five mice. As shown in Figure 7F, the weight of tumors derived from clone 5.3 was smaller than that of tumors derived from naïve HT1080 in four nude mice and, on the fifth mouse, no tumor was observed with clone 5.3 cells. Overall, sh5MP1 reduced the tumor size to 21% of the parent tumor, HT1080 ($P < 0.001$, n = 5). Pathological analysis of tumors isolated from nude mice confirmed that the tumor was fibrosarcoma and that the tumors derived from clone 5.3 contained smaller and fewer dividing cells (Figure 7G). These results indicate that 5MP1 contributes to fibrosarcoma tumorigenicity. Given the significant but minor effect on ATF4 expression, we suggest that *ATF4* is at least one of the many targets of 5MP1. We propose that 5MP1 promotes tumorigenecity through controlling multiple genes with uORFs, including *ATF4*, in their mRNA leader regions (see Discussion).

5MP2 (BZW1) interacts with eIF2 and eIF3 and induces ATF4 expression in human cells

5MP2 is overexpressed in certain types of cancers, and 5MP2 knockdown in salivary mucoepidermoid carcinoma (MEC) reduces its tumorigenicity, implicating 5MP in tumorigenesis (6). However, the molecular target of 5MP2 in tumorigenesis has not been identified. In order to test if 5MP2 overexpression can induce *ATF4*, we generated a pEF1A derivative encoding human 5MP2 and performed the interaction assay by purifying 5MP2 complex II and the *ATF4-luc* reporter assay. As shown in Figure 8A and B, the 5MP2 complex II specifically contained eIF2α and eIF3b (lane 2) as found in the 5MP1 complex II (lane 3). Direct 5MP2 binding to eIF2β was confirmed by isothermal titration calorimetry (ITC), demonstrating a tight binding affinity of $K_D = 1.5$ μM, comparable to the reported affinity for 5MP1 or eIF5 binding to the same protein (11,14) (Figure 8C).

We found that the 5MP2 overexpression induced ATF4 expression by 3-fold in HEK293T (Figure 8D, panel 1). The 5MP2 overexpression reduced protein synthesis similar to 5MP1 (Supplementary Figure S1, column 4), strongly decreased uORF2 translation (Figure 8D, panel 2), indicating uORF2 bypass, but did not decrease the expression

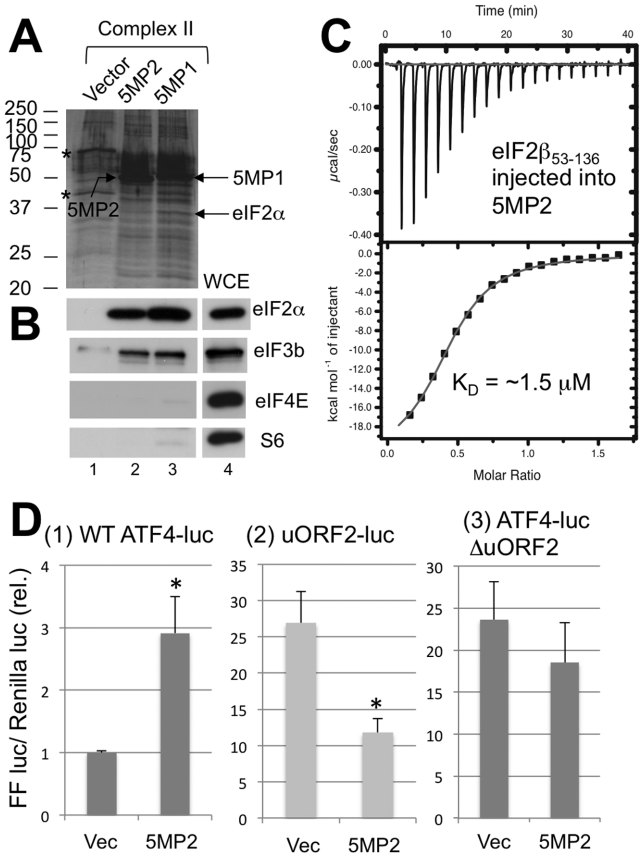

Figure 8. 5MP2/BZW1 reported to be overproduced in certain tumors binds eIF2 and eIF3 and induces ATF4 expression in HEK293T. (**A** and **B**) Single αFLAG affinity purified complexes of 5MP1 and 5MP2 (Complex II) are analyzed by (**A**) silver staining and immunoblotting as in Figure 1. (**C**) ITC assay. Human eIF2β$_{53\text{-}136}$ carrying two K-boxes (161.5 μM), which are the major determinants of interaction with eIF5 (30), was injected into the human 5MP2 sample (20 μM). The ITC experiment was performed as described previously (11,14). (**D**) ATF4- or uORF2-luciferase activities from cells transfected with the indicated reporter plasmid and pEF1A-h5MP2 are measured and presented as in Figure 4A. *, significant changes compared to the value from vector control in each panel. Panel 1, $P = 0.03$ (n = 6). Panel 2, $P = 0.01$ (n = 6).

from *ATF4* ΔuORF2 reporter (Figure 8D, panel 3). This last finding suggests that 5MP2 overexpression does not caused the secondary effect on PIC scanning, which otherwise would compromise the ability of overproduced 5MP2 to induce *ATF4*, as observed with 5MP1 in HEK293T cells (Figure 4A). These results support the notion that 5MP overexpression in general leads to translational induction of *ATF4* in metazoa including both normal and cancerous human cells.

DISCUSSION

The essential roles eIF5 plays in promoting the PIC assembly and accurate translation initiation have been established well in yeast (22,23). However, the role of eIF5 in human biology is underexplored, in particular, in the context of the PIC assembly and regulation, as well as the biological consequence of its overproduction. In this paper, we found for the first time that, similar to yeast, eIF5 overexpression in human cells turns eIF5 into a translation inhibitor (Supplementary Figure S1), thereby inducing *ATF4* translation (Figures 4A, B and 5B). This effect is brought about by the strong ability of eIF5 to bind eIF2, which was demonstrated by our affinity-purification studies (Figure 1). As shown in yeast previously, the overproduced eIF5 not only bound additionally to eIF3 (Figures 1, 3 and Table 1), in support of MFC formation in mammalian cells (8), but also to eIF2B (Table 1), in support of its binding to GDP-bound eIF2 (4,24).

Our finding that 5MP1 binds eIF2 in human cells almost as strongly as eIF2 binds eIF5 (Figure 1) agrees with the previous findings that 5MP1 and eIF5 bind eIF2β-NTT at a similar affinity (11) and thereby compete for eIF2 (5). Our affinity purification study also revealed 5MP1 interaction with eIF1, eIF3 and eIF2B, similar to the results with eIF5-purification studies (Figure 1 and Table 1). It is conceivable that these proteins associate with the 5MP1:eIF2 complex as the core; eIF1 and eIF3 bound through eIF2:GTP:Met-tRNA$_i^{Met}$ TC in a MFC-like complex, and eIF2B bound through eIF2:GDP. Like the eIF5-mediated complexes, formation of these complexes is likely to reduce the TC recruitment and abundance, thereby inducing *ATF4* translation (Figures 4B and 5A and B).

Compared to eIF2 phosphorylation, the ability of overproduced eIF5 or 5MP to induce *ATF4* was weak. This is partly because the overproduced proteins appear to cause a secondary effect through attenuating the PIC scanning in the *ATF4* mRNA leader (Figure 4A, panels 2 and 3). In agreement with this idea, eIF5 overexpression is known to destabilize the scanning competent form of the PIC in yeast and human, thereby allowing mis-initiation from non-AUG codons (25,26). The inhibitory effect of 5MP1 on the scanning PIC is consistent with its binding to eIF3, the ribosome binding factor (5) (Figures 1 and 2), and the fact that 5MP does not possess the GAP function carried by eIF5. Alternatively, the weak effect of eIF5 or 5MP might be due to competition with eIF2B, which can vary depending on the intensity of eIF2αK signaling by an unknown mechanism.

Overexpression of initiation factors, such as eIF4E and eIF3 subunits, and a concomitant increase in cap-dependent mRNA translation have been associated with tumorigenesis (27). In the case of eIF5 and 5MP, their overexpression decreases general translation, but it can contribute to tumorigenesis through enhancing ATF4 expression in favor of tumor survival during stress conditions (hypoxia and nutritional deprivation) encountered by cancer cells in their development and metastasis (28). Our 5MP1-knockdown studies on fibrosarcoma (Figure 7) supports this hypothesis. In regard to the role of 5MP and eIF5 in tumorigenesis, the following questions remain unanswered: Precisely how do these proteins promote *ATF4* translation? How is the intensity of *ATF4* induction regulated in different cell types and conditions? Is overexpression necessary for 5MPs to promote tumorigenesis? Finally, is *ATF4* the sole target of this regulation? For the 5MP expression levels in cancer, while 5MP2 (BZW1) was overexpressed in salivary mucoepidermoid carcinoma, the level of 5MP1 or 5MP2 was equivalent to eIF2 level in the breast carcinoma cell line MCF7 (12). We also confirmed that the levels of 5MP1 and 5MP2 in fibrosarcoma HT1080 are similar to those in HEK293T (HH and KA, personal observations). Furthermore, consistent with 5MP1-knockdown studies in fibrosarcoma, we showed previously that RNAi-mediated knockdown of 5MP in the red flour beetle (the sole copy in the organism) attenuates transcription from a ATF4-dependent gene (11). Therefore, the expression of 5MP at its normal level (not necessarily its overexpression) may contribute to a basal-level ATF4 expression. We also do not know the significance of tissue-specific expression patterns of 5MP1 and 5MP2 from transcriptomics studies (11). As for the number of potential 5MP targets, the recent ribosome profiling study showed that eIF2 inhibition leads to up-regulation of translation of a subset of genes with uORFs in their mRNA leader region (29). These genes include *ATF4*, *ATF5* (the paralog of *ATF4*), and the eIF2α phosphatase *GADD34* and are potentially regulated by 5MP. More works regarding the role of eIF5 and 5MP in cancer biology will add new insights into the development of cancer therapies through translational control.

SUPPLEMENTARY DATA

Supplementary Data are available at NAR Online.

ACKNOWLEDGEMENT

The authors are indebted to Shigeo Hayashi and Reiko Nakagawa (RIKEN Kobe Proteomics Facility) for expertise in MS experiments on complex II fractions and Yoshihiko Fujita for initial analysis of and advice on immunocytochemistry data. The authors also thank Erin Adamson for comments on the manuscript, Ivan Topisirovic and Toshinobu Fujiwara for discussion, Takuya Ohshima, Jacob Morris and Pia Kuhlmann for technical help.

FUNDING

Innovative Award from Terry Johnson Cancer Center, KSU; KU-COBRE Protein Structure and Function Pilot Grant [P30GM110761]; NSF Research Grant [1412250 to K.A.]; Visiting Professorship from Biosignal Research Center, Kobe University (to U.K.); JSPS Short-term Fellowship for Foreign Scientist Invitation (to H. M.); C.K. was

a Merial-NIH Veterinary Research Scholar; S.H. and C.M. are K-INBRE scholars [P20GM103418]. Funding for open access charge: NSF [1412250].
Conflict of interest statement. None declared.

REFERENCE

1. Sonenberg,N. and Hinnebusch,A.G. (2009) Regulation of translation initiation in eukaryotes: mechanisms and biological targets. *Cell*, **136**, 731–745.
2. Harding,H.P., Zhang,Y., Zeng,H., Novoa,I., Lu,P.D., Calfon,M., Sadri,N., Yun,C., Popko,B., Paules,R. *et al.* (2003) An integrated stress response regulates amino acid metabolism and resistance to oxidative stress. *Mol. Cell*, **11**, 619–633.
3. Vattem,K.M. and Wek,R.C. (2004) Reinitiation involving upstream ORFs regulates ATF4 mRNA translation in mammalian cells. *Proc. Natl. Acad. Sci. U.S.A.*, **101**, 11269–11274.
4. Singh,C.R., Lee,B., Udagawa,T., Mohammad-Qureshi,S.S., Yamamoto,Y., Pavitt,G.D. and Asano,K. (2006) An eIF5/eIF2 complex antagonizes guanine nucleotide exchange by eIF2B during translation initiation. *EMBO J.*, **25**, 4537–4546.
5. Singh,C.R., Watanabe,R., Zhou,D., Jennings,M.D., Fukao,A., Lee,B.-J., Ikeda,Y., Chiorini,J.A., Fujiwara,T., Pavitt,G.D. *et al.* (2011) Mechanisms of translational regulation by a human eIF5-mimic protein *Nucleic Acids Res.*, **39**, 8314–8328.
6. Li,S., Chai,Z., Li,Y., Liu,D., Bai,Z., Li,Y., Li,Y. and Situ,Z. (2009) BZW1, a novel proliferation regulator that promotes growth of salivary mucoepidermoid carcinoma. *Cancer Lett.*, **284**, 86–94.
7. Asano,K., Clayton,J., Shalev,A. and Hinnebusch,A.G. (2000) A multifactor complex of eukaryotic initiation factors eIF1, eIF2, eIF3, eIF5, and initiator $tRNA^{Met}$ is an important translation initiation intermediate in vivo. *Genes Dev.*, **14**, 2534–2546.
8. Sokabe,M., Fraser,C.S. and Hershey,J.W. (2012) The human translation initiation multi-factor complex promotes methionyl-tRNAi binding to the 40S ribosomal subunit. *Nucl Acids Res.*, **40**, 905–913.
9. Jennings,M.D. and Pavitt,G.D. (2010) eIF5 has GDI activity necessary for translational control by eIF2 phosphorylation. *Nature*, **465**, 378–381.
10. Huang,H., Yoon,H., Hannig,E.M. and Donahue,T.F. (1997) GTP hydrolysis controls stringent selection of the AUG start codon during translation initiation in *Saccharomyces cerevisiae*. *Genes Dev.*, **11**, 2396–2413.
11. Hiraishi,H., Oatman,J., Haller,S., Blunk,L., McGivern,B., Morris,J., Papadopoulos,E., Guttierrez,W., Gordon,M., Bokhari,W. *et al.* (2014) Essential role of eIF5-mimic protein in animal development is linked to control of ATF4 expression. *Nucleic Acids Res.*, **42**, 10321–10330.
12. Schwanhäusser,B., Busse,D., Li,N., Dittmar,G., Schuchhardt,J., Wolf,J., Chen,W. and Selbach,M. (2011) Global quantification of mammalian gene expression control. *Nature*, **473**, 337–342.
13. Zhang,P. and Samuel,C.E. (2007) Protein kinase PKR plays a stimulus- and virus-dependent role in apoptotic death and virus multiplication in human cells. *J. Virol.*, **81**, 8192–8200.
14. Luna,R.E., Arthanari,H., Hiraishi,H., Nanda,J., Martin-Marcos,P., Markus,M., Arabayov,B., Milbradt,A., Luna,L.E., Seo,H.-C. *et al.* (2012) The C-terminal domain of eukaryotic initiation factor 5 promotes start codon recognition by its dynamic interplay with eIF1 and eIF2β *Cell Rep.*, **1**, 689–702.
15. Uno,S. and Masai,H. (2011) Efficient expression and purification of human replication fork-stabilizing factor, Claspin, from mammalian cells: DNA-binding activity and novel protein interactions. *Genes Cells*, **16**, 842–856.
16. Sadaie,M., Shinmyozu,K. and Nakayama,J.-I. (2008) A conserved SET domain methyltransferase, set11, modifies ribosomal protein Rpl12 in fission yeast. *J Biol Chem*, **283**, 7185–7195.
17. Ishihama,Y., Oda,Y., Tabata,T., Sato,T., Nagasu,T., Rappsilber,J. and Mann,M. (2005) Exponentially modified protein abundance index (emPAI) for estimation of absolute protein amount in proteomics by the number of sequenced peptides per protein. *Mol. Cell. Proteomics*, **4**, 1265–1272.
18. Rehwinkel,J., Behm-Ansmant,I., Gatfield,D. and Izaurralde,E. (2005) A crucial role for GW182 and the DCP1:DCP2 decapping complex in miRNA-mediated gene silencing. *RNA*, **11**, 1640–1647.
19. Jennings,M.D., Zhou,Y., Mohammad-Qureshi,S.S., Bennett,D. and Pavitt,G.D. (2013) eIF2B promotes eIF5 dissociation from eIF2•GDP to facilitate guanine nucleotide exchange for translation initiation. *Genes Dev.*, **27**, 2696–2707.
20. Luna,R.E., Arthanari,H., Hiraishi,H., Akabayov,B., Tang,L., Cox,C., Markus,M.A., Luna,L.E., Ikeda,Y., Watanabe,R. *et al.* (2013) The interaction between eukaryotic initiation factor 1A and eIF5 retains eIF1 within scanning preinitiation complexes. *Biochemistry*, **52**, 9510–9518.
21. Ye,J., Kumanova,M., Hart,L.S., Sloane,K., Zhang,H., De Panis,D., Bobrovnikova-Marjon,E., Diehl,J.A., Ron,D. and Koumenis,C. (2010) The GCN2-ATF4 pathway is critical for tumor cell survival and proliferation in response to nutrient deprivation. *EMBO J.*, **29**, 2082–2094.
22. Hinnebusch,A.G. (2014) The scanning mechanism of eukaryotic translation initiation. *Annu. Rev. Biochem.*, **83**, 779–812.
23. Asano,K. (2014) Why is start codon selection so precise in eukaryotes? *Translation*, **2**, e28387.
24. Singh,C.R., Udagawa,T., Lee,B., Wassink,S., He,H., Yamamoto,Y., Anderson,J.T., Pavitt,G.D. and Asano,K. (2007) Change in nutritional status modulates the abundance of critical pre-initiation intermediate complexes during translation initiation in vivo. *J. Mol. Biol.*, **370**, 315–330.
25. Nanda,J.S., Cheung,Y.-N., Takacs,J.E., Martin-Marcos,P., Saini,A.K., Hinnebusch,A.G. and Lorsch,J.R. (2009) eIF1 controls multiple steps in start codon recognition during eukaryotic translation initiation. *J. Mol. Biol.*, **394**, 268–285.
26. Loughran,G., Sachs,M.S., Atkins,J.F. and Ivanov,I.P. (2011) Stringency of start codon selection modulates autoregulation of translation initiation factor eIF5. *Nucleic Acids Res.*, **40**, 2998–2906.
27. Silvera,D., Formenti,S.C. and Schneider,R.J. (2010) Translational control in cancer. *Nat. Rev. Cancer*, **10**, 254–266.
28. Wek,R.C. and Staschke,K.A. (2010) How do tumors adapt to nutrient stress? *EMBO J.*, **29**, 1946–1947.
29. Andreev,D.E., O' Connor,P.B.F., Fahey,C., Kenny,E.M., Terenin,I.M., Dmitriev,S.E., Cormican,P., Morris,D.W., Shatsky,I.N. and Baranov,P.V. (2015) Translation of 5′ leaders is pervasive in genes resistant to eIF2 repression. *eLife*, **4**, e03971.
30. Asano,K., Krishnamoorthy,T., Phan,L., Pavitt,G.D. and Hinnebusch,A.G. (1999) Conserved bipartite motifs in yeast eIF5 and eIF2Be, GTPase-activating and GDP-GTP exchange factors in translation initiation, mediate binding to their common substrate eIF2. *EMBO J.*, **18**, 1673–1688.